Elemental Analysis of Silicon in Plant Material with Variable-Pressure SEM

Tara L. Nylese,[1]* Adam Berry,[2] and Shannon Oscher[3]
[1]EDAX, A Division of Ametek, Materials Analysis Division, 91 McKee Dr., Mahwah, NJ 07430
[2]Cornell University, Olin Hall, Ithaca, NY 14850
[3]Bergen County Academies, 200 Hackensack Ave., Hackensack, NJ 07601
*Tara.Nylese@ametek.com

Introduction

The cellular structure of biological plant material has been well characterized by light and electron microscopy [1]. Scanning electron microscopy (SEM) uses an electron beam to scan the surface of a sample to study the external morphology of plant cells, tissues, and organs [2]. Analytical SEM beam conditions are typically tailored to the requirements of the sample being investigated, and in the case of biological plant specimens, a low-kV electron beam (1 to 5 kV) is routinely employed for sample surface imaging to reduce beam damage to the tissue. For certain analyses, as in this work, it is necessary to work at non-conventional operating conditions in order to fully characterize the materials being studied by energy dispersive X-ray spectrometry (EDS). By varying the SEM beam conditions, inorganic phases can be located either at the top surface or in the sub-surface regions of plant tissue.

Microscopic investigations of primary plant structures reveal details about plant structural morphology that helps the analyst better understand the functionality of each of the organelles. For example, SEM studies of onion root tips with freeze etching preparation show the location and morphology of the cell wall, nucleus, and nuclear pores [3]. More detailed studies of the double membrane, inner membrane space, and other metabolic compartments are used to understand the processes of photorespiration and amino acid synthesis [4]. Chloroplasts play a very important role in plant tissues for primary life-sustaining functions such as photosynthesis. Studies with SEM and transmission electron microscopy (TEM) show the morphology of chloroplasts and other sub-micron components, such as the inner and outer membranes and the individual thylakoids [4]. The cytoskeleton of the plant cell consists of a network of fibrous actin filaments and microtubules that provide important functions such as cytoplasmic organization, cell division, cell growth, and cell differentiation.

Adaptive Mechanisms in Plants

A secondary function of plant cell structure is to support the organism's ability to adapt to adverse conditions. One example of specialized adaptation is how a plant can maintain its structural integrity even in low-water environments or during periods of drought. In these cases, the organic materials of the plant tissue may not contain adequate hydration to maintain the form and rigidity required for a plant to maintain an erect disposition necessary to gather light for photosynthesis. Therefore, the plant may uptake certain materials in soil or sand to add to its structural integrity. Another example of an adaptive mechanism found in plants is the use of materials for defensive purposes, such as protection from the chewing teeth of herbivores. When a plant contains an abrasive material such as silica, an animal that eats it will suffer breakdown in tooth enamel because of the silicon, and therefore it will avoid eating this type of plant [5].

Equisetum hyemale, commonly referred to as horsetail, is a perennial herbaceous plant with a wide distribution throughout North America. *E. hyemale* is a basal vascular plant, originating in the Devonian period, and it is found in dense clusters throughout the Yellowstone River valley of Montana in wet, forested areas at elevations from 900 to 1500 m (3,000–5,000 ft). It is the single surviving genus of an entire taxonomic group equivalent to angiosperms. Although the species is described as having a bamboo-like appearance due to its hollow core, it is only distantly related to bamboo, which evolved after the end of Cretaceous extinction [6]. The morphology of horsetail includes jointed stems with each stem segment having longitudinal ridges and valleys, as well as a hollow core making up much of the stem internal volume.

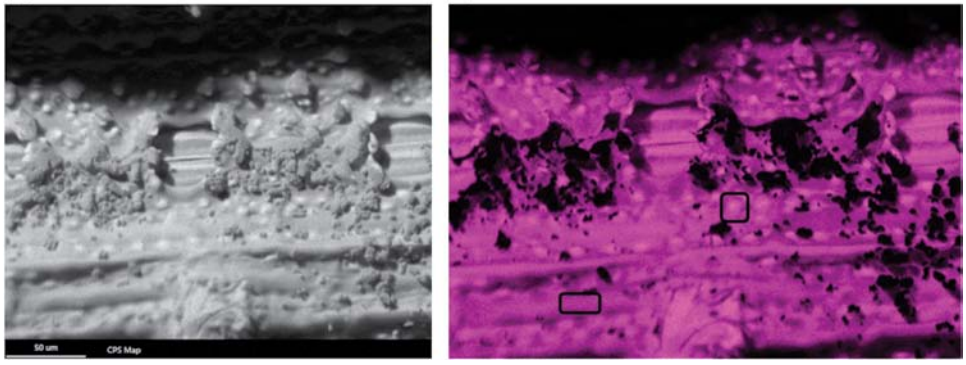

Figure 1: (a) Phytoliths of silica are visible in *Equisetum hyemale* as "knobs" in this X-ray map of silicon as seen in the CPS map showing a useful X-ray view that highlights topography and the locations of more intense X-ray emission, e.g., the silicon in the phytolith "knobs" within the box on the right. (b) Si X-ray image, which shows (in boxes) representative areas of the silicon-rich knob and general plant tissue. Each phytolith is approximately 10 µm. Image width = 275 µm.

https://doi.org/10.1017/S155192951500005X Published online by Cambridge University Press

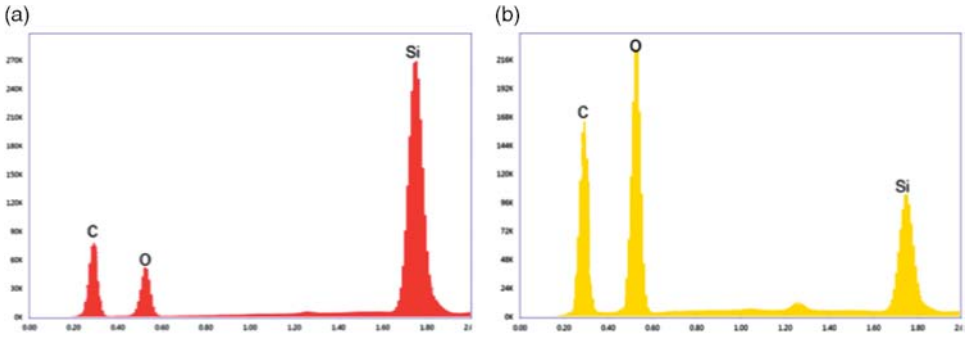

Figure 2: EDS spectra extracted from a phase map of the phytolith (red) shows higher Si intensity than surrounding areas (yellow). Carbon is highly prevalent due to the depth of the electron beam and effects of the low-vacuum environment. The relative differences in the C and O peaks are likely due to the beam spread, which includes contribution from surrounding material.

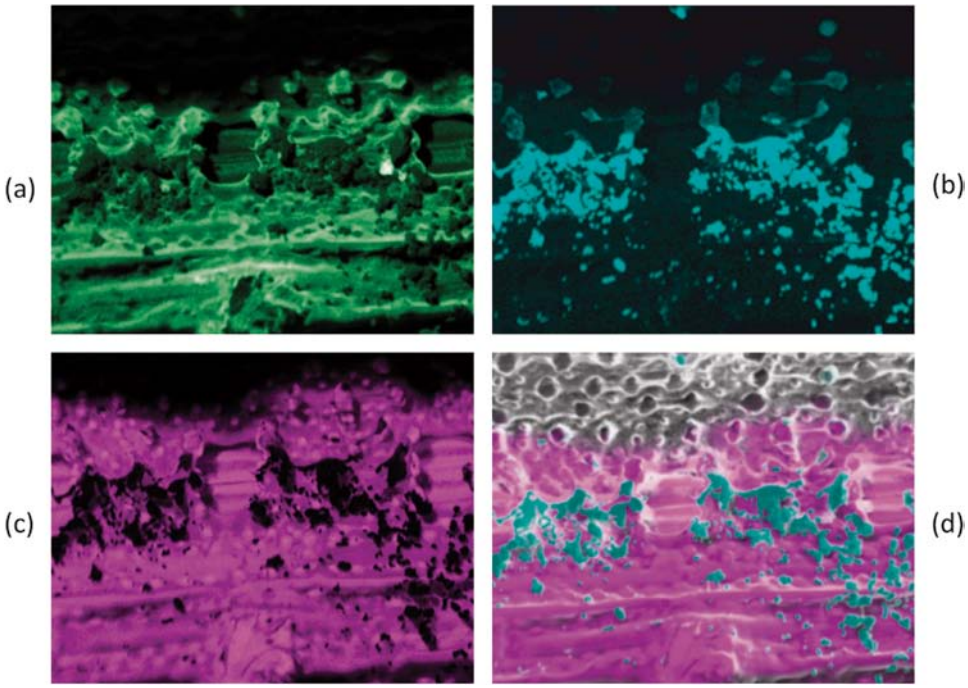

Figure 3: Element maps for (a) carbon (green), (b) calcium (blue), (c) silicon (magenta), and (d) overlay of the Si and Ca maps collected at 10 kV over the SEM image. Image width = 275 µm.

Horsetail is the only vascular plant where silicon provides vital functions, both as an essential mineral element [7] and as a factor in structural integrity [8]. The presence and distribution of silicon within horsetail has been described as varied, occurring on the epidermal surface of the entire cell wall primarily as discrete knobs and rosettes [9]. The morphology of these structures, including their presence and distribution, is not well documented by microscopic or microanalytical methods, particularly in comparison to the number of studies performed on the primary life-sustaining tissue structures. Therefore, investigations into the local chemical distribution of silicon within the horsetail plant tissue should provide needed information on the structural mechanisms at play.

Cladium masriscus, commonly known as saw-tooth sedge or sedge grass, belongs to a species of flowering plants with long grass-like leaves that have a hard, rough, and serrated edge. *Cladium jamaicense* is a sawgrass that is typically located in North America, whereas *C. mariscus* tends to be located in Europe. The amount of Si present in these types of grasses has previously been measured in amounts between 0.4%–1% of the dry mass of the plant, with variations noted between developing and mature leaves [10]. Once present in the vascular tissue of the plant, the silicon forms silica bodies known as phytoliths [11] that associate with the cell wall and lumina [12] as amorphous silica. A general study of silicon deposition in 15 plant species found that the storage and arrangement of silicon in the plants can have varied shapes including oval, dumb-bell, and saddle-shaped [13]. However, this is not fully understood and is an area for further exploration. This article describes the results of the elemental analyses of these structures.

Materials and Methods

Operating conditions. The most notable aspect of the present investigation was the use of analytical SEM conditions outside the typical conditions for biological analyses. Traditional SEM analysis of soft materials emphasizes two main aspects of the electron beam, namely the kV and the beam current. A low kV beam, below 5 kV, and sometimes 1 kV or less, is used to limit the electron penetration depth to the uppermost surface in order to reveal surface detail. Also, a low beam current is used to reduce sample beam damage and charge retention within the non-conductive tissue. These conditions allow image acquisition, however, they pose a challenge for elemental analysis by X-ray spectrometry because of the weak X-ray signals generated. A benefit of X-ray analysis is that X rays have deeper escape depth compared to electrons. Therefore, X-ray analysis can be used to study subsurface features within a material. A higher kV electron beam is required to penetrate to these depths, so appropriate sample preparation and handling are necessary to counteract beam damage and charging in the material. One method is to coat the sample with a conductive material to carry the negative surface charge to electrical ground, and a second is to introduce a gas into the SEM chamber, which can be ionized to produce positive ions that can neutralize the negative surface charge.

Neutralizing charge with a chamber gas. When first attempting the work of finding silicon in the plant tissue, the

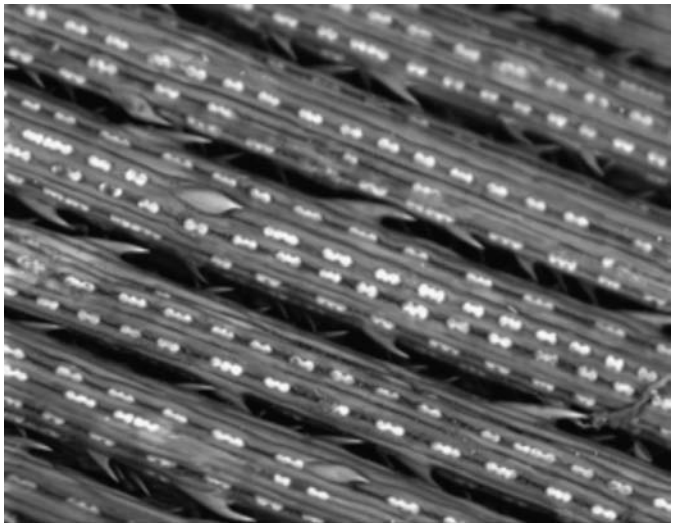

Figure 4: BSE image at 10 kV with the silicon-containing dumbbell-shaped bodies clearly visible throughout the length of the blade. Image width = 410 µm.

traditional approach was followed, simply out of convention. Unfortunately, that analysis attempt, on an unprepared section of a blade of sedge grass at a low kV in a field-emission SEM, failed to highlight the presence of silicon in X-ray spectrometry analyses along the flat surface of the grass blade. Further, at this operating condition, the sample showed excessive charging, preventing quality imaging and analysis. However, a second attempt followed a less conventional set of conditions, using an electron beam of 10 kV and introducing 40 Pa ambient air pressure in a Hitachi S3400N variable-pressure SEM with an EDAX Octane Pro (10 mm^2) silicon drift detector (SDD). While the increased chamber gas pressure increases the electron beam spread and generates X rays from a wider area causing a diffuse appearance of the X-ray map, this mode of operation permits use of the higher beam energy to penetrate further into the sample for subsurface analysis. Although X-ray mapping in variable-pressure mode suffers reduced image quality due to the beam spread issue, this approach allows acquisition of images and data when they are otherwise not possible [14]. This set of operating conditions highlighted the presence of silicon while mitigating sample charging and damage.

Silicon drift detector. Typically a large-area SDD is used for analysis of biological materials; however, in this case a small-area SDD could be employed because the combination of higher beam energy and a short sample-to-detector distance produced sufficient X-ray signal. A further benefit of this detector was its superior Mn Kα energy resolution of 124 eV, which helps to separate overlapping peaks. Paired with ultra-fast pulse processing electronics, the collected signal was efficiently converted into useable data for spectrum and mapping collection.

Spectrum imaging. Spectrum imaging is a data acquisition method in which a spectrum is stored at each pixel in the image, creating an *x-y-E* data cube. The data cube is then interrogated by proprietary software designed to map the phases in the materials. The TEAM EDS phase mapping routine uses an EDAX exclusive algorithm that permits phase matching in real time, immediately from the first map pass, as well as in post-collection mode on a stored data cube. The routine accomplishes the following: (1) evaluates the elements in each spectrum of a map data set, (2) measures each element's X-ray peak intensity as determined by a region of interest fit method, (3) compares ratios of all elements together, and (4) finally makes a determination of the phases present from those elemental ratios. If all element ratios are the same or similar to within ± 5% between any two or more pixels, the pixels will be grouped into the same phase and displayed as the same color in the phase map image. Any pixel whose spectrum does not match within the tolerance range is assigned as a new phase and displayed as a different color. This process continues throughout the collection, refining the results, as more intensity data are added. Because phase determination is based directly on the spectrum peak intensities, there is no requirement for intermediate element map image generation to increase the quality of the phase matching, even with limited intensity information. During collection, an auto-fit routine

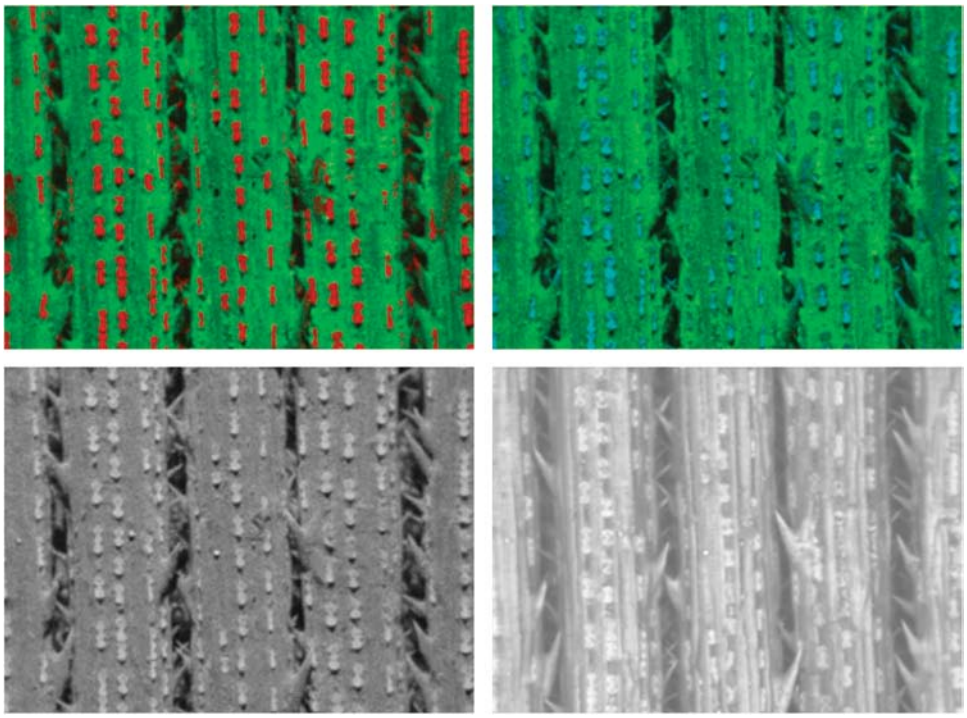

Figure 5: Composite elemental maps of the sawgrass sample (top images) with organic carbon (green), silicon (red), and oxygen (cyan). Images below are the X-ray CPS image (lower left) and the BSE electron image (lower right). Image width = 510 µm.

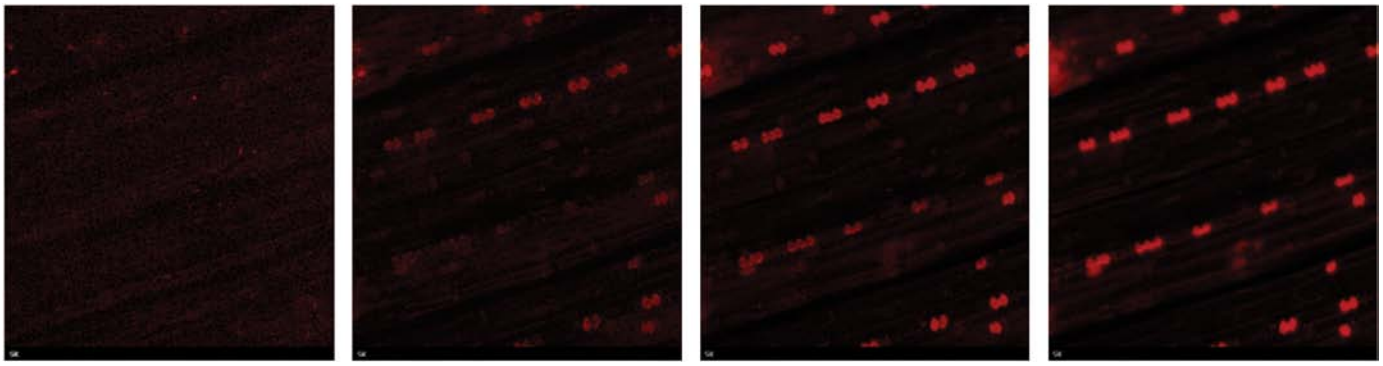

Figure 6: Series of silicon maps at increasing electron-accelerating voltage (5, 10, 15, 20 kV) showing increased signal intensity as the beam energy increases. Image width = 250 µm.

dynamically adjusts the default tolerance range, preventing the assignment of multiple phases that are closely similar.

While the phase selection and discrimination criteria described above are automatic, manual mode is possible so the desired phase spectrum may be collected and added by the user either before or after the collection. Automatically selected phase spectra can also be edited by the user, as a semi-automated mode of phase matching. All phase spectra are saved with the data cube and can be adjusted as needed. The result of phase mapping is a comprehensive phase image, which represents the chemical distribution of elements within a sampling area.

Depth of X-ray generation. Once the X-ray spectra confirmed the presence of silicon in both the horsetail and the sawgrass, further experimentation with different operating conditions demonstrated that changes in beam energy can characterize the location and depth of the silicon. Data collection at increasing beam energies on the sawgrass was performed to study the relationship between silicon intensity and beam penetration depth.

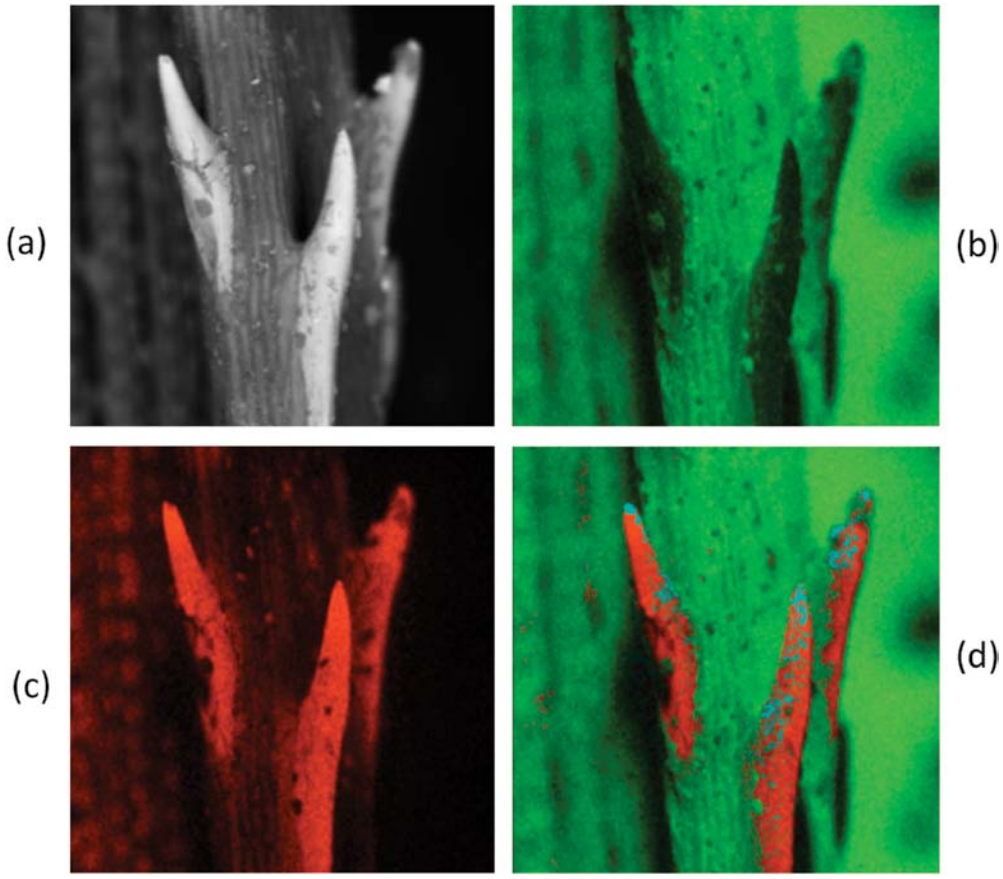

Figure 7: Edge of the saw grass spiky thorns. (a) BSE image, (b) organic carbon (green), (c) silicon (red) image, and (d) composite image showing the silicon-rich spikes decorated with an oxygen-rich phase (light blue). Image width = 1560 µm.

Results

Horsetail shoot. Results from the horsetail shoot sample show variations in the distribution and intensity for silicon and other elements within the organic material. Figure 1a shows an SEM image of the specimen surface with "knobs" of silica (phytoliths). This SEM imaging view, known as the counts per second (CPS) map, was produced using collected X rays rather than electrons. It displays a gray-level intensity representation of the summed X-ray signals. This image highlights X-ray signal intensity differences and can be valuable for explaining variations related to topography or excitation effects. Figure 1b shows the relative distribution of Si in a map of the same area. Figure 2 shows spectra from the two different phases (within boxes in Figure 1b) with higher Si peak intensity from the phytoliths in the red spectrum and higher C and O intensities in the area away from the phytoliths. X-ray maps of the additional elements detected are shown in Figure 3, which also includes a combined element map overlay.

Sawgrass. A flat blade of sawgrass was also characterized

at the same 10 kV SEM beam energy. In contrast to conventional imaging work below 5 kV, in the 10 kV analysis the silica bodies were immediately visible in the backscattered electron (BSE) image, Figure 4. EDS maps were then collected to confirm that the dumbbell shaped bodies were, in fact, rich in silicon, as expected. Figure 5 confirms the presence of these characteristic features.

Initial work for this analysis demonstrated that by increasing the beam from 5 kV to 10 kV the signal from Si became stronger. The increase in Si signal can indicate greater X-ray generation, a subsurface location for the Si-rich dumbbells, or both. The next step was to increase the beam energy incrementally to collect data from increasingly deeper locations within the plant tissue. The sequence shown in Figure 6 demonstrates an increasing silicon X-ray signal intensity as the beam probes deeper. Another notable result was that the clarity and resolution of the morphology of the silica storage bodies became clearer, likely because of the increased signal generated by the brighter electron beam.

Figure 7 shows a BSE image of serrated edge thorns, visible on the side of the blade, along with elemental maps that confirm the spines are silicon-rich (red) within the organic carbon material (green). A light blue phase in the composite X-ray map was identified as oxygen.

Discussion

The X-ray maps obtained in this study were particularly important because the results supported the research on the expected morphology of subsurface inorganic materials. There has been limited imaging characterization of these materials in prior work, most likely because of the need for nontraditional operating conditions. It was only in a follow-up attempt that the analyst changed the original conditions to a higher kV to check for the presence of silicon, which yielded successful results. Technology has also progressed, allowing this type of work to be more practical in SEM high-beam-current capability, in EDS detector sensitivity, and in X-ray processing efficiency. Therefore this was an important step in learning more about subdermal elemental distribution in plant systems.

Conclusion

Micro-features of plant systems can be characterized and more completely visualized and understood using site-specific elemental sampling with EDS in the SEM. The low-vacuum conditions of the SEM, combined with higher beam energy and efficient X-ray processing, allow enhanced analysis of silicon in plant materials. Increased electron beam energy reveals structures that are not visible at or near the surface of the plant sample and that are not detectable when using traditional conditions. Serial collection at increasing beam energies shows increasing silicon signal intensity and indicates that the silicon is located below the surface of the plant tissue.

Acknowledgments

Special thanks to Stanley M. Wiatr, Chair, Biological & Physical Sciences, Montana State University, for initiating the EDS X-ray analysis of horsetail shoots in Spring 2012, which lead to the original work *Microscopic Chemical Characterization of Silicon in Biological Plant Materials,* presented as a poster at the MRS Fall Symposium in 2012.

References

[1] JL Hall and C Hawes, *Electron Microscopy of Plant Cells*, Academic Press Limited, London, 1991.
[2] OL Gamborg et al., (eds), *Plant Cell, Tissue and Organ Culture*, Springer-Verlag, Berlin Heidelberg, 1995.
[3] TE Weier et al., *Botany: An Introduction to Plant Biology*, Wiley, New York, 1974.
[4] Atwell et al., *Plants in Action*, MacMillian, Sydney, 1999.
[5] J. W. Hunt et al., *Ann Bot* 102(4) (2008) 653–56.
[6] RL Hauke, *Nova Hedwigia* (8) (1963) 1–123.
[7] E Epstein, *Annu Rev Plant Phys* 50 (1999) 641–64.
[8] PB Kaufman et al., *Am J Bot* 58 (1971) 309–16.
[9] HA Currie and CC Perry, *Annals of Botany* 100(7) (2007) 1383–89.
[10] K Klančnik, *J Photochem Photobiol B* 130 (2014) 1–10.
[11] PB Kaufman et al., *Ann Bot-London* 55 (1985) 487–507.
[12] CJ Prychid et al., *Bot Rev* 69 (2004) 377–40.
[13] FC Lanning, *Ann Bot-London* 64 (1989) 395–10.
[14] DE Newbury, *J Res Natl Inst Stan* 107 (2002) 567–603.

MT